

Stochastic Phased Array Performance Indicators for Quality-of-Service-Enhanced Massive MIMO

Noud Kanters¹ and Andrés Alayón Glazunov^{1,2}

¹Department of Electrical Engineering, University of Twente, 7500AE Enschede, Netherlands.

²Department of Science and Technology, Linköping University, Bredgatan 33, 602 21 Norrköping, Sweden.

Email: n.b.kanters@utwente.nl

In this paper, we show that the signal-to-interference-plus-noise ratio (SINR) at a base station (BS) equipped with an arbitrary physical array antenna can be expressed as a function of two fundamental figures-of-merit (FoMs): (I) the instantaneous effective gain (IEG), and (II) the beamforming-channel correlation (BCC). These two FoMs are functions of the array antenna layout, the antenna elements, the propagation channel and the applied signal processing algorithms, and hence they are random variables (RVs) in general. We illustrate that both FoMs provide essential insights for quality-of-service (QoS)-based phased array design by investigating their statistics for BSs applying full-digital (FD) zero forcing (ZF) beamforming. We evaluate various array designs and show that arrays with higher IEGs and a reduced probability of low BCCs can increase the ergodic sum rate and reduce the need for scheduling.

Introduction: Phased array antennas are a key component of base stations (BSs) in multi-user wireless communication systems. Traditionally, they are configured along a uniform half-wavelength-spaced lattice to prevent grating lobes. Recently, however, communication-oriented array design [1] has shown that unconventional layouts can enhance the user equipment (UE) quality-of-service (QoS). Examples of considered QoS-based key performance indicators (KPIs) are ergodic channel capacity [2], signal-to-interference-plus-noise ratio (SINR) [3, 4], or SINR-dependent metrics like bit error rate [5] and ergodic sum rate [5–8]. However, understanding the physical phenomena behind array-layout-induced QoS improvements is complicated, as is illustrated by, for instance, conflicting statements on whether mutual coupling (MC) enhances or deteriorates ergodic channel capacity; see, e.g., [9] and references therein. Typically, different assumptions are made regarding the number and type of antenna elements, the number of served UEs, and the propagation channel model. Moreover, conventional channel normalization may partially hide the impact of the element type, its element pattern, and impedance matching. This hinders the straightforward comparison of the proposed array designs. Conventional phased array KPIs like sidelobe-level and beamwidth provide limited insight into how an array will perform in a multi-user system, especially in channels with a non-line-of-sight (NLoS) component. Hence, generalized KPIs incorporating the effects of the array, the channel and signal processing are needed. In this work, we derive such KPIs. Specifically, we show that the SINR in single-cell systems solely depends on the transmit powers and two random variables (RVs): (I) the instantaneous effective gain (IEG) and (II) the beamforming-channel correlation (BCC). This result is obtained by normalizing the BS-UE channels based on a BS reference array. Subsequently, we illustrate how the array design can affect the statistics of these two RVs, and with that also of QoS-based array design objectives. To this end, we consider BSs equipped with various linear arrays applying full-digital (FD) zero forcing (ZF) beamforming, both with and without user scheduling, and we analyse how the statistics of the two RVs affect the achieved SINR and ergodic sum rate.

Massive MIMO System Model: Let's consider a single-cell massive multiple-input-multiple-output (MIMO) system comprising a BS serving K UEs. Each UE has a single antenna element, whereas the BS has an N -element phased array antenna. The narrowband uplink received signal $\mathbf{y}^{\text{UL}} \in \mathbb{C}^N$ is defined as in, e.g., [10] and reads

$$\mathbf{y}^{\text{UL}} = \sum_{k=1}^K \sqrt{p_k} \mathbf{h}_k x_k + \sigma_{\text{UL}} \mathbf{n}, \quad (1)$$

where $\mathbf{h}_k \in \mathbb{C}^N$, p_k and $x_k \sim \mathcal{N}_{\mathbb{C}}(0, 1)$ represent the BS-UE channel vector, the transmit power and the data signal for the k^{th} UE, respectively. Moreover, $\mathbf{n} \sim \mathcal{N}_{\mathbb{C}}(\mathbf{0}_N, \mathbf{I}_N)$ is the receiver noise vector and σ_{UL}^2 the noise power. Assuming the BS applies linear receive combining using combining matrix $\mathbf{W} \in \mathbb{C}^{N \times K} = [\mathbf{w}_1 \ \dots \ \mathbf{w}_K]$, it follows that the instantaneous uplink SINR for UE k equals

$$\text{SINR}_k^{\text{UL}} = \frac{p_k |\mathbf{w}_k^H \mathbf{h}_k|^2}{\underbrace{\sum_{i=1, i \neq k}^K p_i |\mathbf{w}_k^H \mathbf{h}_i|^2}_{\text{Intra-Cell Interference}} + \underbrace{\sigma_{\text{UL}}^2 \|\mathbf{w}_k\|^2}_{\text{Noise}}}. \quad (2)$$

SINR-Dependent QoS-based Array Design Single-Cell Systems: In this section, we present the channel normalization technique assumed in the remainder of this paper. We use this to derive a novel expression for the SINR in single-cell systems. The result applies to arbitrary array layouts, arbitrary linear combining algorithms, and arbitrary channel models.

Before computing the SINR in (2), some form of norm-based normalization is generally applied to $\mathbf{h}_1, \dots, \mathbf{h}_K$ to have control over the signal-to-noise ratio (SNR). Conventional normalization approaches are $\|\mathbf{h}_k\| = \sqrt{N} \ \forall k = 1, \dots, K$ or $\|\mathbf{H}\|_F = \sqrt{NK}$, where $\mathbf{H} = [\mathbf{h}_1 \ \dots \ \mathbf{h}_K]$. However, when designing physical array antennas based on a QoS-metric like the SINR, the impact of the antennas is typically embedded in the channel vectors $\mathbf{h}_1, \dots, \mathbf{h}_K$, see, e.g., [2, 5]. Applying these conventional normalization techniques cancels out essential information regarding the relation between, on the one hand, deterministic array aspects like MC and impedance matching and, on the other hand, the stochastic propagation environment in which the array is deployed. Consequently, assessing the performance of various array designs deployed within a certain channel or of a specific array deployed in different channels is not straightforward. To circumvent this problem, we propose normalizing the BS-UE channels relative to a reference array rather than in an absolute sense. Hence, the normalized channel between the BS and UE k is defined as

$$\tilde{\mathbf{h}}_k = \sqrt{N_{\text{ref}}} \frac{\mathbf{h}_k}{\|\mathbf{h}_k^{\text{ref}}\|}, \quad (3)$$

where we use $\tilde{\mathbf{h}}$ and \mathbf{h} to differentiate between non-normalized channels and their normalized counterparts as used in (2), respectively. $\mathbf{h}_k^{\text{ref}}$ represents the BS-UE channel that would be observed if the BS array of interest were replaced by the reference array while leaving the propagation channel (defined by parameters like, e.g. angles-of-arrival (AOAs), complex path gains and Rice factor) unchanged. N_{ref} is the number of elements in the reference array. The reference array does not need the same number of elements as the array of interest. Note that the normalized channel between a UE and the reference array by definition satisfies $\|\mathbf{h}_k^{\text{ref}}\| = \sqrt{N_{\text{ref}}}$. Although not required, we consider reference arrays composed of isotropic elements in this work.

Assuming that $p_1 = \dots = p_K = P_{\text{UL}}/N_{\text{ref}}$ and applying (3), it follows that (2) can be written as

$$\text{SINR}_k^{\text{UL}} = \frac{P_{\text{UL}} G_k^{\text{ie}} |\omega_{kk}|^2}{\underbrace{P_{\text{UL}} \sum_{i=1, i \neq k}^K G_i^{\text{ie}} |\omega_{ki}|^2}_{\text{Intra-Cell Interference}} + \underbrace{1}_{\text{Noise}}}, \quad (4)$$

where we have assumed without loss of generality that $\sigma_{\text{UL}} = 1$, and where we've introduced the complex-valued BCC coefficient ω_{ki} and the IEG G_i^{ie} . Here, ω_{ki} is defined as

$$\omega_{ki} = \frac{\mathbf{w}_k^H \mathbf{h}_i}{\|\mathbf{w}_k\| \|\mathbf{h}_i\|}, \quad (5)$$

which satisfies $0 \leq |\omega_{ki}|^2 \leq 1$ for $i \in \{1, \dots, K\}$. From (5), it follows that $|\mathbf{w}_k^H \mathbf{h}_i|^2 = |\omega_{ki}|^2 \|\mathbf{w}_k\|^2 \|\mathbf{h}_i\|^2$. This is substituted in (2), whereupon we have used that $p_i \|\mathbf{h}_i\|^2 = \frac{P_{\text{UL}}}{N_{\text{ref}}} \|\sqrt{N_{\text{ref}}} \frac{\mathbf{h}_i}{\|\mathbf{h}_i^{\text{ref}}\|}\|^2 = P_{\text{UL}} \frac{\|\mathbf{h}_i\|^2}{\|\mathbf{h}_i^{\text{ref}}\|^2} = P_{\text{UL}} \frac{\|\mathbf{h}_i\|^2}{\|\mathbf{h}_i^{\text{ref}}\|^2} = P_{\text{UL}} G_i^{\text{ie}}$, where the last steps follow from (3) and from the definition of the IEG, i.e.,

$$G_i^{\text{ie}} = \frac{\|\mathbf{h}_i\|^2}{\|\mathbf{h}_i^{\text{ref}}\|^2}. \quad (6)$$

Hence, in the definition of the IEG, the numerator represents the instantaneous channel gain observed at the physical BS array under consideration, whereas the denominator represents, for the same UE and the same propagation channel, the instantaneous channel gain observed at the reference array. Therefore, the IEG measures the channel gain of an array of physical elements relative to an isotropic array with no MC. It is worthwhile to note that an expression similar to (4) is obtained for the downlink when assuming that the downlink transmit power is defined as $p_i \|\mathbf{w}_i\|^2 = P_{\text{DL}}/N_{\text{ref}}$ for all $i \in \{1, \dots, K\}$. In this case, expressions for uplink and downlink SINR are equivalent if $P_{\text{UL}} = P_{\text{DL}}$. For the sake of conciseness, we only focus on the uplink.

The principle behind SINR-dependent QoS-based array layout design in single-cell systems can be understood from (4). The stochastic propagation channel, the deterministic BS array antenna, and the applied signal processing algorithms (e.g., user scheduling and beamforming) jointly determine the statistics of the coefficients G_k^{ie} and $|\omega_{ki}|^2$, $i \in \{1, \dots, K\}$. Both coefficients are RVs in general, and consequently, $\text{SINR}_k^{\text{UL}}$ is an RV as well. Through proper design of the array antenna, the probability distributions of G_k^{ie} and $|\omega_{ki}|^2$ can be shaped to optimize the design objective, which is typically a specific statistic of (a function of) $\text{SINR}_k^{\text{UL}}$.

Channel Model and Signal Processing: The theory presented in this paper applies to arbitrary channel models. However, we limit ourselves to pure line-of-sight (LoS) far-field channels for conciseness. Furthermore, we assume that all antenna elements are purely vertically polarized. The UEs use isotropic antennas, whereas the BS uses a physical array antenna. Hence, the channel between UE k and the BS can be represented as [11]

$$\tilde{\mathbf{h}}_k = \mathbf{a}(\phi_k, \theta_k) \quad (7a)$$

$$= \mathbf{g}(\phi_k, \theta_k) \odot \mathbf{a}_{\text{isotropic}}(\phi_k, \theta_k) \quad (7b)$$

$$= \mathbf{C}_{\text{oc}}(\phi_k, \theta_k) \mathbf{a}_{\text{isotropic}}(\phi_k, \theta_k), \quad (7c)$$

where $\mathbf{a}(\phi_k, \theta_k)$ is the analytic array manifold [11] at (ϕ_k, θ_k) , the azimuth and elevation AOs for UE k . The tilde in $\tilde{\mathbf{h}}_k$ indicates that this is the channel vector before normalization according to (3). In (7b) and (7c), $\mathbf{a}_{\text{isotropic}}(\phi, \theta) \in \mathbb{C}^N$ represents the array's steering vector (SV) defined as

$$\mathbf{a}_{\text{isotropic}}(\phi, \theta) = \begin{bmatrix} \exp(-j \frac{2\pi}{\lambda} \mathbf{r}_1 \cdot \mathbf{u}(\phi, \theta)) \\ \vdots \\ \exp(-j \frac{2\pi}{\lambda} \mathbf{r}_N \cdot \mathbf{u}(\phi, \theta)) \end{bmatrix}, \quad (8)$$

where λ is the wavelength, $\mathbf{r}_n \in \mathbb{R}^3$ represents the position of element n in space in Cartesian coordinates, and $\mathbf{u}(\phi, \theta) = [\cos(\phi) \cos(\theta), \sin(\phi) \cos(\theta), \sin(\theta)]^T$ is a unit vector in the direction of (ϕ, θ) . The impact of the physical antenna elements is modelled using embedded element patterns (EEPs) [12] in (7b) and using a mutual coupling matrix (MCM) in (7c). Specifically, the vector $\mathbf{g}(\phi, \theta) \in \mathbb{C}^N$ is defined as $\mathbf{g}(\phi, \theta) = [g_1(\phi, \theta) \cdots g_N(\phi, \theta)]^T$, where $g_n(\phi, \theta)$ represents the EEP of element n , whereas $\mathbf{C}_{\text{oc}}(\phi, \theta)$ is the direction-dependent MCM defined as [11]

$$\mathbf{C}_{\text{oc}}(\phi, \theta) = \mathbf{Z}_L (\mathbf{Z} + \mathbf{Z}_L)^{-1} \mathbf{G}_{\text{oc}}(\phi, \theta). \quad (9)$$

Here, $\mathbf{Z} \in \mathbb{C}^{N \times N}$ is the mutual impedance matrix, $\mathbf{Z}_L \in \mathbb{C}^{N \times N}$ is the load impedance matrix, and $\mathbf{G}_{\text{oc}}(\phi, \theta) \in \mathbb{C}^{N \times N}$ is a diagonal matrix defined as

$$\mathbf{G}_{\text{oc}}(\phi, \theta) = \text{diag}([g_{\text{oc},1}(\phi, \theta), \dots, g_{\text{oc},N}(\phi, \theta)]), \quad (10)$$

where $g_{\text{oc},n}(\phi, \theta)$ is the open-circuit element pattern of element n , i.e., the pattern of element n when embedded in the array with all other elements open-circuited.

A convenient simplification of (9) exists for BS arrays composed of thin dipoles with inter-element spacings larger than quarter-wavelength [13]. For these arrays, dipole elements behave as minimum scattering antennas, meaning their open-circuit patterns are approximately equivalent to the isolated element patterns, see, e.g., [14]. Since isolated dipoles are omni-directional in the plane orthogonal to the dipole axis, it follows that for an array of identical dipole elements oriented vertically in a horizontal plane, $\mathbf{G}_{\text{iso}}(\phi, \theta) \propto \mathbf{I}_N$. Hence, the MCM (9) becomes

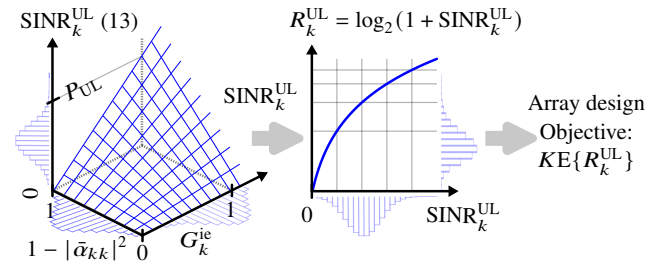


Fig 1 Ergodic sum rate-based array design for FD ZF single-cell systems.

Table 1. Antenna Elements

Element	Manifold	Element Pattern
1	Isotropic (8)	-
2	$\lambda/2$ -Dipole (7c)	$g_{\text{oc},n}(\phi, \theta) \propto \frac{\sin(\frac{\pi}{2} \sin(\theta))}{\cos(\theta)}$ [18]
3	Cosine (7b)	$g_n(\phi, \theta) \propto \begin{cases} \cos(\phi) \cos(\theta) & \phi \leq 90^\circ \\ 0 & \text{otherwise.} \end{cases}$

$\mathbf{C}_{\text{iso}} \propto \mathbf{Z}_L (\mathbf{Z} + \mathbf{Z}_L)^{-1}$ and is therefore direction-independent. For a BS array of isotropic elements, we can set $\mathbf{g}(\phi, \theta) = \mathbf{1}_N$ in (7b) and define

$$\tilde{\mathbf{h}}_{\text{isotropic}} = \tilde{\mathbf{h}}(\mathbf{g}(\phi, \theta) = \mathbf{1}_N) = \mathbf{a}_{\text{isotropic}}(\phi, \theta), \quad (11)$$

where we have omitted the subscript k for ease of notation.

Assuming perfect channel state information (CSI) is available at the BS, the ZF combining matrix is computed as $\mathbf{W} = \mathbf{H}(\mathbf{H}^H \mathbf{H})^{-1}$ [10, 15]. By definition, the ZF combining vector for UE k , \mathbf{w}_k , is orthogonal to the (intra-cell) interference subspace I_k , i.e., the vector space spanned by the $K-1$ channel vectors \mathbf{h}_i , $i \in \{1, \dots, K\} \setminus k$ [16]. Hence, for ZF combining, the beamforming-channel correlation satisfies $|\omega_{ki}|^2 = 0$ for all $i \in \{1, \dots, K\} \setminus k$, meaning the interference term in the denominator of (4) vanishes. Moreover, it follows from [17] that

$$|\omega_{kk}|_{\text{ZF}}^2 = 1 - |\cos(\bar{\gamma}_{kk})|^2 = 1 - |\bar{\alpha}_{kk}|^2, \quad (12)$$

where $\bar{\gamma}_{kk}$ represents the generalized angle between \mathbf{h}_k and its projection on I_k , and where $|\bar{\alpha}_{kk}|^2$ represents the corresponding generalized spatial correlation coefficient (GSCC) which can be computed using, e.g., the Gram-Schmidt procedure [17]. Hence, for ZF combining, (4) reduces to

$$\text{SINR}_k^{\text{UL}}|_{\text{ZF}} = P_{\text{UL}} G_k^{ie} (1 - |\bar{\alpha}_{kk}|^2). \quad (13)$$

Fig. 1 visualizes the array design procedure for ergodic sum rate-based design in the case of BSs applying FD ZF combining.

Numerical Simulations and Simulation Parameters: We focus on BSs applying FD ZF combining. Since ZF causes low SINRs in the case of highly correlated BS-UE channels [8], we consider scenarios without and with user scheduling. Specifically, we apply user dropping according to [19]. A correlation threshold of $\frac{|\mathbf{h}_i^H \mathbf{h}_j|}{\|\mathbf{h}_i\| \|\mathbf{h}_j\|} \leq 0.45$ is considered in the scenario with dropping. The considered array antenna elements are presented in Table 1. The reference array for computing the IEG is a $\lambda/2$ -spaced uniform linear array (ULA) composed of isotropic elements. Furthermore, we consider two arrays composed of vertically oriented half-wave dipoles: a ULA and a non-uniform linear array (NULA). The Tchebyshev parametrization of [6] determines the spatial configuration of the latter. For both dipole arrays, each dipole is terminated in the complex conjugate of its self impedance Z_s such that $\mathbf{Z}_L = Z_s^* \mathbf{I}_N$ in (9). The mutual and self impedances are defined in, e.g., [18]. Finally, we consider the same NULA but with synthetic cosine elements; see Table 1. These elements have a directive element pattern and could thus represent, for instance, patch antennas. For all arrays, except for the reference array, we consider two (average) inter-element spacings: $d_{\text{avg}} = \lambda/2$ and $d_{\text{avg}} = 2\lambda$. All arrays are composed of $N = N_{\text{ref}} = 32$ elements. We scale the element patterns by a factor γ such that the integrals of their received gain patterns in the absence of MC are equal. Hence, for the dipoles, we apply $\int_{-\pi}^{\pi} \int_{-\pi/2}^{\pi/2} |\gamma \frac{Z_s}{Z_s + Z_s} g_{\text{oc},n}(\phi, \theta)|^2 \cos(\theta) d\theta d\phi =$

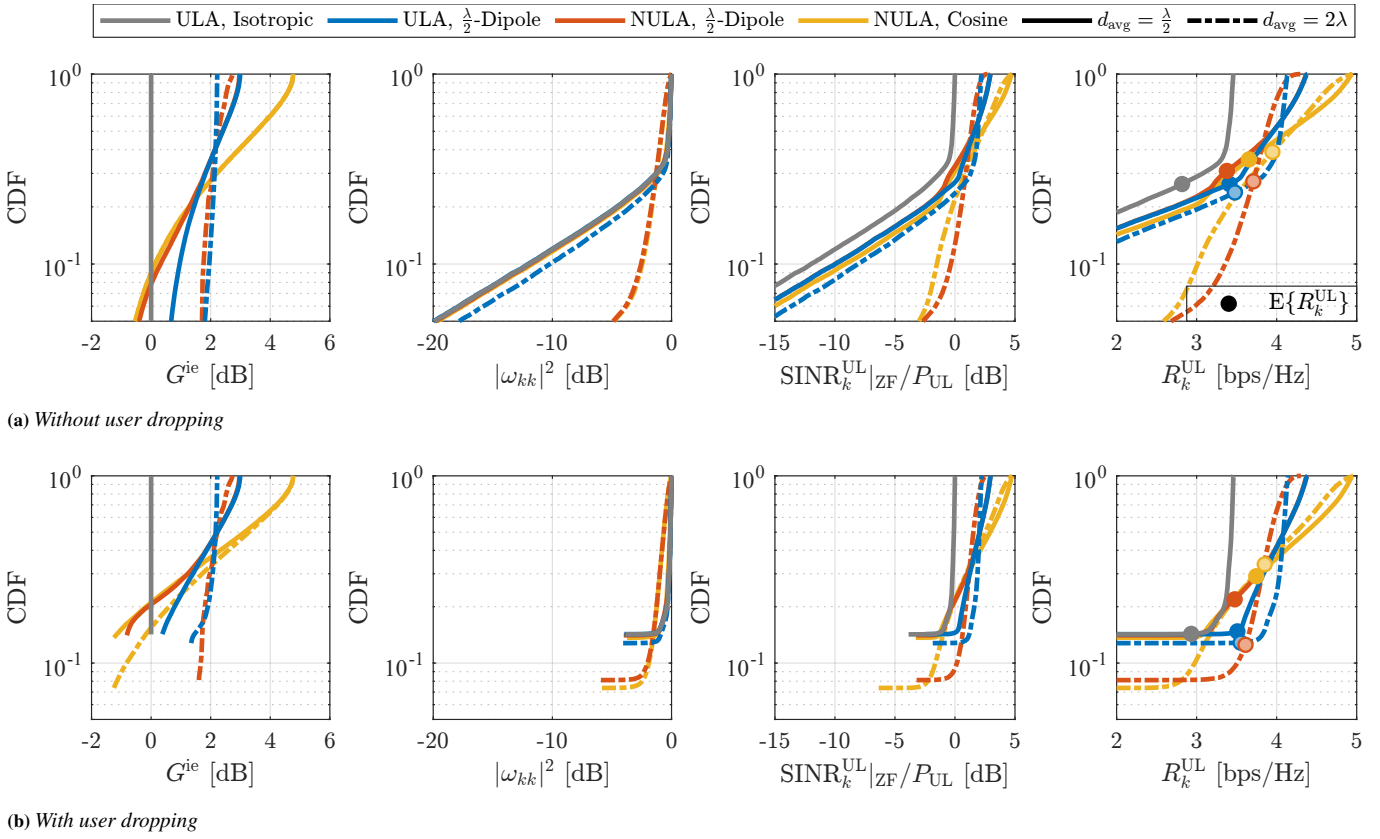


Fig 2 From left to right: CDFs of (I) IEG G_k^{ie} (6); (II) ZF BCC $|\omega_{kk}|^2|_{\text{ZF}}$ (12); (III) $\text{SINR}_k^{\text{UL}}|_{\text{ZF}}/P_{\text{UL}}$ (13); and (IV) UE rate $R_k^{\text{UL}} = \log_2(1 + \text{SINR}_k^{\text{UL}}|_{\text{ZF}})$ at $P_{\text{UL}} = 10$ dB.

4π , ultimately resulting in the well-known 2.15 dBi gain in the horizontal plane [18]. Note that the impedance ratio appearing in the integral can alternatively be taken into account by introducing a factor $\frac{Z_s + Z_s^*}{Z_s}$ in the definition of the MCM, see, e.g., [14]. For the cosine elements, we apply $\int_{-\pi}^{\pi} \int_{-\pi/2}^{\pi/2} |\gamma g_n(\phi, \theta)|^2 \cos(\theta) d\theta d\phi = 4\pi$. We consider a 2-dimensional horizontal geometry with a BS serving $K = 8$ UEs, which are uniformly distributed over a 120° sector. The azimuth and elevation AOA are defined as $\phi_k \sim U(-60^\circ, 60^\circ)$ and $\theta_k = 0^\circ$, $k = 1, \dots, K$, respectively. We simulate 10^4 realizations with BS-UE channels modelled as (7), or as (11) for the isotropic reference array.

Results: Results are presented in Fig. 2a and Fig. 2b for the scenarios without and with user dropping, respectively. They are discussed below.

The first subplots of Fig. 2a and Fig. 2b show, in dB-scale, the cumulative distribution functions (CDFs) of the IEG G_k^{ie} (6). The percentile at which a graph ends in Fig. 2b indicates the probability of a user being dropped. Clearly, this probability is the lowest for the NULAs with $d_{\text{avg}} = 2\lambda$. Looking at the served (i.e., non-dropped) UEs alone, it can be seen that user dropping has a negligible impact on the statistics of the IEG G_k^{ie} . Furthermore, it is observed that the isotropic reference array has an IEG of 0 dB. This is expected, as it represents the gain of the reference array relative to itself. On the contrary, for the dipole arrays, the IEGs vary. Variations are larger for $\lambda/2$ -spaced arrays than for 2λ -spaced arrays. At large spacings, the MC becomes negligible, and hence the EEPs become approximately equal to isolated dipole patterns, which are omni-directional with a gain of 2.15 dBi. At small spacings, however, the MC shapes the EEPs such that the gain towards a certain UE depends on its AOA. The cosine elements achieve the highest IEGs for both inter-element spacings. However, they also come with the largest variations inherent to their directive element patterns.

The second subplots of Fig. 2a and Fig. 2b show, in dB-scale, the CDFs of the ZF BCC $|\omega_{kk}|^2$ (13). Contrary to what was observed for G_k^{ie} , user dropping has a significant impact on the statistics of $|\omega_{kk}|^2$ of the served UEs: it reduces the variation drastically. Moreover, it is observed that for the considered array antennas, $|\omega_{kk}|^2$ is determined to a great extent by the array layout, whereas the element type has only

a small effect. Finally, it is observed that in the scenario without user dropping, the 2λ -spaced NULAs significantly reduce the probability of having a low BCC. The same arrays also provide a lower probability of dropping users. In the case of ZF combining, a high GSCC $|\bar{a}_{kk}|^2$, and thus a low BCC $|\omega_{kk}|^2$ (12), implies that suppressing the intra-cell interference of the k^{th} UE causes the k^{th} UE itself to be suppressed as well, ultimately resulting in low SINRs. To reduce the probability of having high GSCCs, one could apply scheduling (here, user dropping). However, as can be concluded from Fig. 2, one could also exploit the array layout, thereby reducing the dropping probability.

The third subplots show the CDFs of $\text{SINR}_k^{\text{UL}}|_{\text{ZF}}$. As expected, they show great correspondence to the individual CDFs of the IEG and the BCC. The resulting UE rates R_k^{UL} are presented in the fourth subplots for $P_{\text{UL}} = 10$ dB. The dots indicate the average UE rates $E\{R_k^{\text{UL}}\}$ (computed with the UE rate of a dropped UE set to 0), such that the ergodic sum rate is found through multiplication by K . From the arrays considered in this work, the 2λ -spaced NULAs achieve the highest ergodic (sum) rate in the scenario without user dropping. Since the UE rate is a concave function of the SINR (Fig. 1), it intuitively follows that arrays providing a low probability of low $\text{SINR}_k^{\text{UL}}$ benefit the ergodic sum rate. Although the latter can also be accomplished by employing signal processing (here, user dropping), Fig. 2b shows that NULAs are still beneficial since they reduce the probability of a user being dropped. Since the cosine element arrays provide the largest IEGs, the 2λ -spaced NULA of cosine elements can be considered the optimal array from the ones considered here.

Conclusions and Future Work: It has been shown that SINR-dependent QoS-based array design in single-cell systems is a matter of shaping the probability distributions of two RVs, i.e., the IEG and the BCC. The concept is illustrated in detail for a FD ZF system, for which the latter is merely a function of the GSCC. It is shown that ergodic sum rate enhancements reported for unconventional array layouts mainly result from a reduced probability of a high GSCC and that such arrays can reduce the need for scheduling. In the future, we plan to use the presented concepts to design new array layouts rather than analyzing existing ones.

References

1. Oliveri, G., Gottardi, G., Massa, A.: A new meta-paradigm for the synthesis of antenna arrays for future wireless communications. *IEEE Transactions on Antennas and Propagation* 67(6), 3774–3788 (2019)
2. Amani, N., et al.: Sparse array synthesis including mutual coupling for mu-mimo average capacity maximization. *IEEE Transactions on Antennas and Propagation* (2022)
3. Bencivenni, C., et al.: Effects of regular and aperiodic array layout in multi-user mimo applications. In: 2017 IEEE International Symposium on Antennas and Propagation & USNC/URSI National Radio Science Meeting, pp. 1877–1878. IEEE (2017)
4. Aslan, Y., Roederer, A., Yarovoy, A.: System advantages of using large-scale aperiodic array topologies in future mm-wave 5g/6g base stations: An interdisciplinary look. *IEEE Systems Journal* 16(1), 1239–1248 (2021)
5. Ge, X., et al.: Multi-user massive mimo communication systems based on irregular antenna arrays. *IEEE Transactions on Wireless Communications* 15(8), 5287–5301 (2016)
6. Pinchera, D., et al.: Antenna arrays for line-of-sight massive mimo: Half wavelength is not enough. *Electronics* 6(3), 57 (2017)
7. Amani, N., et al.: Multi-panel sparse base station design with physical antenna effects in massive mu-mimo. *IEEE Transactions on Vehicular Technology* 69(6), 6500–6510 (2020)
8. Farsaei, A., et al.: Uniform linear arrays with optimized inter-element spacing for los massive mimo. *IEEE Communications Letters* 25(2), 613–616 (2020)
9. Chen, X., Zhang, S., Li, Q.: A review of mutual coupling in mimo systems. *Ieee Access* 6, 24706–24719 (2018)
10. Björnson, E., et al.: Massive mimo networks: Spectral, energy, and hardware efficiency. *Foundations and Trends® in Signal Processing* 11(3-4), 154–655 (2017)
11. Friedlander, B.: Antenna array manifolds for high-resolution direction finding. *IEEE Transactions on Signal Processing* 66(4), 923–932 (2017)
12. Pozar, D.M.: The active element pattern. *IEEE Transactions on Antennas and Propagation* 42(8), 1176–1178 (1994)
13. Craeye, C., González-Ovejero, D.: A review on array mutual coupling analysis. *Radio Science* 46(02), 1–25 (2011)
14. Clerckx, B., et al.: Impact of antenna coupling on 2×2 mimo communications. *IEEE Trans. Veh. Technol.* 56(3), 1009–1018 (2007)
15. Marzetta, T.L.: *Fundamentals of massive MIMO*. Cambridge University Press (2016)
16. Björnson, E., Bengtsson, M., Ottersten, B.: Optimal multiuser transmit beamforming: A difficult problem with a simple solution structure [lecture notes]. *IEEE Signal Processing Magazine* 31(4), 142–148 (2014)
17. Lin, H.C.: Spatial correlations in adaptive arrays. *IEEE Transactions on Antennas and Propagation* 30(2), 212–223 (1982)
18. Balanis, C.A.: *Antenna theory: analysis and design*. John Wiley & sons (2015)
19. Yang, H., Marzetta, T.L.: Massive mimo with max-min power control in line-of-sight propagation environment. *IEEE Transactions on Communications* 65(11), 4685–4693 (2017)